LA-UR- 11-00764

Approved for public release; distribution is unlimited.

Title: A Class of Ejecta Transport Test Problems

Author(s):
James E. Hammerberg, XCP-5
William T. Buttler, P-23
David M. Oro, P-23
Christopher L. Rousculp, XCP-6
Christopher Morris, P-25
Fesseha G. Mariam, P-25

Intended for: NECDC 2010 CONFERENCE
LOS ALAMOS
OCT. 18-22, 2010

Los Alamos
NATIONAL LABORATORY
EST. 1943

Los Alamos National Laboratory, an affirmative action/equal opportunity employer, is operated by the Los Alamos National Security, LLC for the National Nuclear Security Administration of the U.S. Department of Energy under contract DE-AC52-06NA25396. By acceptance of this article, the publisher recognizes that the U.S. Government retains a nonexclusive, royalty-free license to publish or reproduce the published form of this contribution, or to allow others to do so, for U.S. Government purposes. Los Alamos National Laboratory requests that the publisher identify this article as work performed under the auspices of the U.S. Department of Energy. Los Alamos National Laboratory strongly supports academic freedom and a researcher's right to publish; as an institution, however, the Laboratory does not endorse the viewpoint of a publication or guarantee its technical correctness.

Form 836 (7/06)

A Class of Ejecta Transport Test Problems (U)

J.E. Hammerberg, W.T. Buttler , D.M. Oro, C. Rousculp, C. Morris, and F. Mariam

Los Alamos National Laboratory, Los Alamos, NM 87545

Hydro code implementations of ejecta dynamics at shocked interfaces presume a source distribution function of particulate masses and velocities, $f_0(m,v;t)$. Some of the properties of this source distribution function have been determined from extensive Taylor and supported wave experiments on shock loaded Sn interfaces of varying surface and subsurface morphology. Such experiments measure the mass moment of f_0 under vacuum conditions assuming weak particle-particle interaction and, usually, fully inelastic capture by piezo-electric diagnostic probes. Recently, planar Sn experiments in He, Ar, and Kr gas atmospheres have been carried out to provide transport data both for machined surfaces and for coated surfaces.

A hydro code model of ejecta transport usually specifies a criterion for the instantaneous temporal appearance of ejecta with source distribution $f_0(m,v;t_0)$. Under the further assumption of separability, $f_0(m,v;t_0) = f_1(m)f_2(v)$, the motion of particles under the influence of gas dynamic forces is calculated. For the situation of non-interacting particulates, interacting with a gas via drag forces, with the assumption of separability and simplified approximations to the Reynolds number dependence of the drag coefficient, the dynamical equation for the time evolution of the distribution function, $f(r,v,m;t)$, can be resolved as a one-dimensional integral which can be compared to a direct hydro simulation as a test problem. Such solutions can also be used for preliminary analysis of experimental data. We report solutions for several shape dependent drag coefficients and analyze the results of recent planar dsh experiments in Ar and Xe. (U)

Introduction

The evolution of material which is produced in shock wave experiments when a strong shock impinges on a free surface or at a surface in contact with a gas is a complex process. The size and velocity distribution of this material for ductile metals depends upon the initial surface roughness, the strength and time dependence of the shock wave and the nature of the release state which is achieved: solid, liquid, mixed phase, defective, or damaged. Recent experimental data for Sn and other metals [1- 3] as well as large scale NonEquilibrium Molecular Dynamics (NEMD) simulations are beginning to shed light on the microscopic and mesoscopic processes involved and their connections to driven interfacial instabilities [4-5].

Once a distribution of ejected material is produced, its evolution in a shocked gas contiguous to the released metal involves a complex interaction of particles (whose shape, size, and state may be changing), with each other and with the flowing gas. For the general calculation of material transport in a gas, an accurate hydrodynamic code is necessary. Part of the process of assessing the validity of such a calculation includes verification, that is to say assessment of the accuracy of the numerical solution of the hydrodynamic algorithms and models in the code. One aspect of verification includes test problems with known solutions that can be compared with code calculations. In the following sections we present a set of planar test problems for a simple model of transport including only particulate drag with the gas at a shocked interface, given an initial particulate distribution function which is assumed to be separable. The solutions obtained can also be compared with piezo probe measurements [1-3] of the time dependent mass density measured in gas given the experimental time

dependent profiles for the piezo probe response in vacuum. We present comparisons for experiments with a Sn/He interface and a W/Ar and W/Xe interface in which the W interface consists of a compact distribution of micron size particles.

Distribution functions for ejecta transport

We consider the distribution function of particles with position **r**, velocity **v** and mass m, in the volume element **drdv**dm about **r**, **v** and m at time t, denoted by f(**r**,**v**,m;t). The number of particles in this volume element is given by:

$$f(\mathbf{r},\mathbf{v},m;t)d\mathbf{r}d\mathbf{v}dm \ .$$

Within the relaxation time approximation to the Boltzmann equation, f satisfies

$$\frac{\partial f}{\partial t}+\mathbf{v}\cdot\frac{\partial f}{\partial \mathbf{r}}+\frac{\mathbf{F}}{m}\cdot\frac{\partial f}{\partial \mathbf{v}}=\left.\frac{df}{dt}\right|_{scat}=\frac{1}{\tau}df \ . \tag{1}$$

For the case of no scattering we have

$$f(\mathbf{r},\mathbf{v},m;t)=\int\delta(\mathbf{r}-\mathbf{r}(t))\delta(\mathbf{v}-\mathbf{v}(t))f_0(\mathbf{r}_0,\mathbf{v}_0,m)d\mathbf{r}_0d\mathbf{v}_0 \tag{2}$$

where $f_0(\mathbf{r}_0,\mathbf{v}_0,m)$ is the initial distribution function at t=0. The particle positions and velocities **r**(t) and **v**(t) depend implicitly on $\mathbf{r}_0$, $\mathbf{v}_0$ and m via the initial values for the solutions of the equations of motion:

$$\frac{d}{dt}\mathbf{r}(t)=\mathbf{v}(t)\ , \tag{3}$$

$$\frac{d}{dt}\mathbf{v}(t)=\frac{\mathbf{F}}{m}\ , \tag{4}$$

with $\mathbf{r}(0)=\mathbf{r}_0$, and $\mathbf{v}(0)=\mathbf{v}_0$. We restrict our discussion here to the case of no scattering.

Connection to piezo-probe experiments and vacuum solutions

The vacuum experiments of Buttler and Zellner [1-3] measure the force transmitted by the particles to a piezo-electric probe at a distance z from the shocked interface which results in a voltage V(t) at some distance z from the initial interface. The connection between the distribution function f and the experimental pressure P is in general:

$$P(t)=\int f(z,v,m;t)mv^2dmdv \ . \tag{4}$$

For the vacuum situation the expressions in the previous section become

$$f(z,v,m;t)=\int\delta(z-vt)f_0(z_0,v,m)dz_0\ , \tag{5}$$

$$P_0(t)=(\frac{z}{t})^2\left[\frac{1}{t}\int f_0(z_0,\frac{z}{t},m)mdmdz_0\right], \tag{6}$$

$$f_0(z_0,v_0,m)=\frac{1}{A}\delta(z_0)f_0(v_0,m)\ , \tag{7}$$

$$P_0(t) = (\frac{z}{t})^2 \frac{1}{t}\frac{1}{A}\int f_0(\frac{z}{t},m)m dm\,, \tag{8}$$

$$\rho_0(z;t) = \frac{1}{t}\int f_0(z_0,\frac{z}{t},m)m\,dm\,dz_0\,. \tag{9}$$

Thus for zero external field, probe pressure and particle density are related via

$$\rho_0(z;t) = (\frac{z}{t})^{-2} P_0(t)\,. \tag{10}$$

This direct proportionality only holds in the free streaming limit. For the situation in which the particles interact with the gas, this is no longer the case.

Solutions for non-zero external field: particle drag

For nonzero external fields, (2) remains valid but the particulate equations of motion are more complicated. We consider the case of particle drag:

$$\mathbf{F} = -\frac{1}{2}\rho_g C_D A\left|\mathbf{v}-\mathbf{v}_g\right|(\mathbf{v}-\mathbf{v}_g)\,. \tag{11}$$

where C_D is the drag coefficient A is the area in the direction of the propagation velocity and the subscript g denotes gas quantities. We consider expressions for the Reynolds number dependence for shape dependent drag coefficients:

I. General spherical :

$$\begin{aligned} C_D &= \frac{24}{Re}(1+0.167Re^{2/3}) \qquad (Re \le 10^3) \\ C_D &= 0.42 \qquad (Re \ge 10^3) \end{aligned} \tag{12}$$

II. Irregular shape:

$$C_D = 1.4 \tag{13}$$

III. Jet-like:

$$C_D = \frac{2.17}{\sqrt{Re}} \tag{14}$$

where the Reynolds number is defined as

$$Re = \frac{D_p\left|v_p - v_g\right|}{\nu} \tag{15}$$

and ν is the kinematic viscosity defined in terms of the coefficient of viscosity as $\eta = \rho_g \nu$, and D_p and v_p are the particle diameter and velocity.

Writing the solution for z(t) as:

$$z(t,u_0) = v_{fs}t + u_0\tau(t,u_0)$$

equations 3 and 4 may be solved for $\tau(t,u_0)$ with the results:

I. General spherical:

$$\tau(t,u_0)=3t_0B^{-\frac{3}{2}}\left\{\sqrt{B}\left[1-\frac{1}{\sqrt{1+B(1-x^2)}}\right]-\left[\sin^{-1}\left(\sqrt{\frac{B}{1+B}}\right)-\sin^{-1}\left(x\sqrt{\frac{B}{1+B}}\right)\right]\right\} \tag{16}$$

$$B=0.167(Re^{(0)})^{\frac{2}{3}}\ ,\quad x=\exp(-\tfrac{1}{3}\tfrac{t}{t_0})\ ,\quad t_0=\frac{1}{18}\frac{\rho_p D_p^2}{\eta}$$

II. Irregular shape:

$$\tau(t,u_0)=t_b\log(1+\frac{t}{t_b})\ , \tag{17}$$

$$t_b=\frac{24}{C_D}\frac{1}{Re^{(0)}}t_0=0.95\frac{D_p}{u_0}\left(\frac{\rho_p}{\rho_g}\right),$$

III. Jet-like:

$$\tau(t,u_0)=t_b\left[\frac{t/t_b}{1+t/t_b}\right], \tag{18}$$

$$t_b=\frac{22.1}{\sqrt{Re^{(0)}}}t_0=1.7\left(\frac{\rho_p}{\rho_g}\right)^{\frac{1}{2}}\sqrt{\frac{m_p}{\eta u_0}}\ ,$$

where

$$Re^{(0)}=\frac{D_p\left|v_p(t=0)-v_g\right|}{\nu}\ ,\quad m_p=\rho_p\frac{\pi}{6}D_p^3\ , \tag{19}$$

and m_p and ρ_p are the particle mass and density. These trajectories are to be substituted in the right hand side of equation 2.

Separable distribution functions

When the distribution function f_0 is separable, i.e.

$$f_0(\mathbf{v},m)=f_0^{(1)}(\mathbf{v})f_0^{(2)}(m)\ , \tag{20}$$

simplifications can be made and the expressions for ρ and P may be written as a one dimensional integral. The results are given below.

$$\rho(z,t)=\frac{1}{A}\int f_0^{(1)}(v_0(z,t))\frac{1}{\left|\frac{dz}{du_0}\right|_{u_0(z,t)}}f_0^{(2)}(m)mdm \tag{21}$$

$$=\frac{1}{M}z\int P_0\left[\frac{z}{v_0(z,t)}\right]\frac{v_0(z,t)^{-3}}{\left|\frac{dz}{du_0}\right|_{u_0(z,t)}}f_0^{(2)}(m)mdm\ , \tag{22}$$

$$P(t)=\frac{1}{M}z\int P_0[\frac{z}{v_0(z,t)}]\frac{v_0(z,t)^{-3}}{\left|\frac{dz}{du_0}\right|_{u_0(z,t)}}v(t,v_0(z,t))^2 f_0^{(2)}(m)mdm \tag{23}$$

where

$$v_0(z,t) = v_{fs} + u_0(z,t)\,, \tag{24}$$

and $u_0(z,t)$ is the solution of

$$z - v_{fs}t = u_0(z,t)\tau(t,u_0(z,t))\,. \tag{25}$$

The one-dimensional integral is a solution which may be compared with numerical simulations given the initial distribution functions $f_0^{(1)}(v)$ and $f_0^{(2)}(m)$. For cases II and III $u_0(z,t)$ may be solved for analytically. For I it must be obtained numerically except in the case of Stokes drag i.e. low Reynolds number flow when it can be obtained analytically . As an example, we have taken approximate forms for the size distribution and compared to the experimental data for Sn into He gas in the Taylor wave experiments of Buttler et al. using the low Reynolds number limit of case I [6] and an approximate form for the size distribution

$$f_0^{(2)}(D) = N_0\gamma\left(\frac{D}{D_0}\right)^{-(\gamma-1)}\frac{1}{D_0} \quad (D \geq D_0)\,, \tag{26}$$

$$P(z;t)=\left(\frac{\gamma-3}{\gamma}\right)(\lambda t)^{-\frac{1}{2}(\gamma-3)}\int_0^{\lambda t}dx\left(\frac{z}{v}\right)P_0\left(\frac{z}{v}\right)\left[1-\frac{x}{v}\left(\frac{z}{t}-v_{fs}\right)\right]^2\frac{x^{\frac{1}{2}(\gamma-3)}}{(1-\exp-x)} \tag{27}$$

where

$$v = v_{fs} + \frac{x}{(1-\exp-x)}\left(\frac{z}{t} - v_{fs}\right)\,, \qquad \lambda^{-1} = t_0^{[min]} = t_0 = \frac{1}{18}\frac{\rho_p D_0^2}{\eta} \tag{28}$$

The comparison with the experimental data is given is figure 1 for the particle pressure at the piezo-pin. The data are for Sn with a 60 μ-in finish driven with a Taylor wave profile with a shock pressure of 33 GPa. A value of $\gamma = 6$ was chosen for the comparison. The initial He gas pressure was 4 bar.

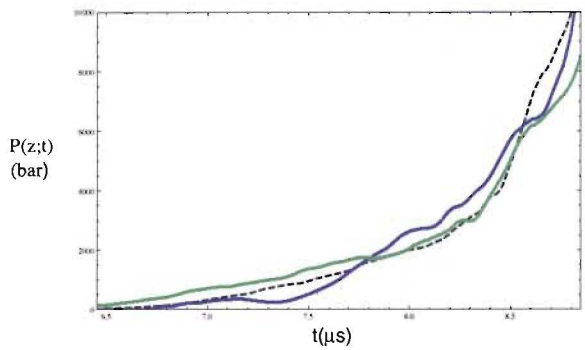

Fig.1 Calculated P(z;t): dashed line. Vacuum P(z;t) data: green line. He gas data: blue line

Transport of W surface ejecta in Ar and Xe

Recent Taylor wave experiments using PRad and piezo-electric probe diagnostics may be analyzed in terms of the above expressions. In these experiments a nearly mono-disperse 40 μm layer of Tungsten particles with diameters between 0.5 and 1.0 was deposited on an Aluminum substrate which was driven with a P25 lens and 16 mm of Calcitol resulting in a free surface velocity of 1.25 km/s. In these experiments the vacuum response and the response in Ar and Xe gases was measured with Lithium Niobate piezo-electric probes and densities were measured with proton radiography at the Los Alamos Neutron Science Center. The initial gas densities were 17 kg/m^3 and the initial temperatures 300 K. Although the size distribution of the W particles has a small dispersion about 1 μm for a preliminary analysis we have taken the mass distribution function $f_0^{(2)}(m)$ above to be a δ-function. In this case the integral for P(t) becomes a simple function of t at the position z of the probe from the free surface given by

$$P(z,t) = \frac{t}{\lambda(z,t)\tau(t)}\left\{1 - \frac{t}{t_0}\frac{1}{\lambda(z,t)}(1 - \frac{v_{fs}t}{z})\right\}^2 P_0(\frac{t}{\lambda(z,t)}), \tag{29}$$

where

$$\lambda(z,t) = 1 + (\frac{t}{\tau(t)} - 1)(1 - \frac{v_{fs}t}{z}), \tag{30}$$

$$\tau(t) = t_0(1 - \exp(-\frac{t}{t_0})). \tag{31}$$

Fig.2 shows a comparison with Ar experimental data for a value of the viscosity of η=119 μPa-s and t_0=9.0 μs

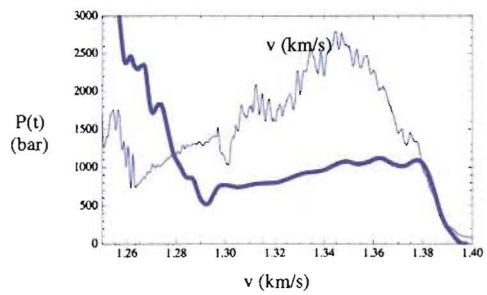

Fig. 2 Vertical scale: Pressure (bar). Horizontal scale: Velocity (km/s). Thick curve: Argon gas experimental data. Thin curve: Calculation assuming Stokes drag using t_0=9.0 μs corresponding to a value of viscosity of 119 μPa-s.

The actual distribution in particle sizes is from 0.5 -1.0 μm and if we assume a broader distribution in particle sizes we obtain a much better fit to the data as seen in Fig. 3 where 50 % of the particles are uniformly distributed at diameters from 0.2 to 0.5 μm.

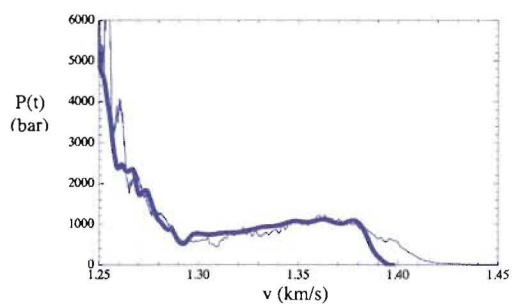

Fig. 3 Vertical scale: Pressure (bar). Horizontal scale: Velocity (km/s). Thick curve: Argon gas experimental data. Thin curve: Calculation assuming a viscosity of 100 μPa-s and a distribution of particle diameters in the ratios 0.1[0.2 μm] +0.1[0.3 μm] + 0.1[0.4 μm] + 0.1[0.5 μm] + 0.5[1 μm].

If the source particle distribution remained the same, the calculated P(t) for Xenon would only depend on the Xe shear viscosity. Fig. 4 shows the comparison with the same mass distribution as Fig.3 for the Xe gas piezo-electric pin data assuming a viscosity of η = 186 μPa-s to fit the leading edge of the distribution.

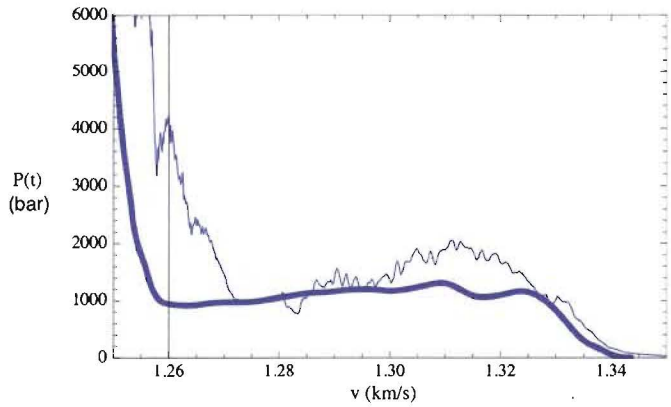

Fig. 4 Vertical scale: Pressure (bar). Horizontal scale: Velocity (km/s). Thick curve: Xenon gas experimental data. Thin curve: Calculation assuming a viscosity of 186 μPa-s and a distribution of particle diameters in the ratios 0.1[0.2 μm] +0.1[0.3 μm] + 0.1[0.4 μm] + 0.1[0.5 μm] + 0.5[1 μm]. Experimental data: Pin 3.

It is evident that the calculation over-predicts the pin data at low velocities which indicates a poor approximation to the mass distribution that may evolve in time. An indication of why this might be so can be found in the Hugoniot state achieved behind the gas shock front. An estimate based upon a strong shock analysis gives gas shock temperatures in Ar and Xe of 3200 K and 9500 K respectively. Since the low pressure melting temperature of W is approximately 3700 K it is likely that the low velocity discrepancy is due to the formation of molten W droplets of smaller size which would shift the low velocity peak to lower velocities. Figure 5 summarizes the analysis for gas transport pin data in Ar and Xe and Fig. 6 includes the vacuum data upon which the analysis is based.

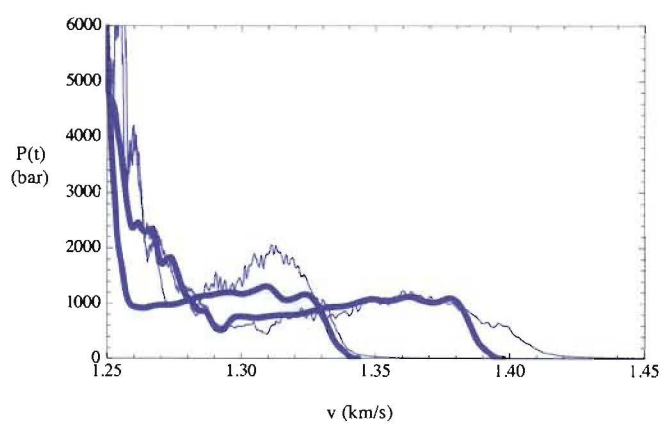

Fig. 5 Vertical scale: Pressure (bar). Horizontal scale: Velocity (km/s). Thick curve: Argon and Xenon gas experimental data. Thin curves: Calculations assuming viscosities of 100 and 186 μPa-s and a distribution of particle diameters in the ratios 0.1[0.2 μm] +0.1[0.3 μm] + 0.1[0.4 μm] + 0.1[0.5 μm] + 0.5[1 μm]. Experimental data: Argon – Pin 1 and Xenon - Pin 3.

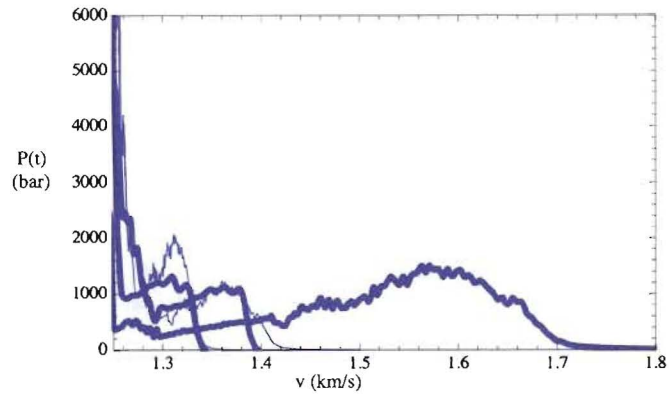

Fig. 6 Vertical scale: Pressure (bar). Horizontal scale: Velocity (km/s). Same as Fig.5 with the vacuum pin pressure (pin 1) shown. Experimental data; heavy lines.

Discussion

We have presented a set of solutions for the time dependent distribution function for the transport of particles ejected into a gas from a shocked interface under the assumption that the distribution function is separable. Solutions have been presented for the case of particulate drag for different particle shapes and expressions have been derived for the particle density as a function of spatial coordinate and time and for the piezo-electric probe response at position z as a function of time. These expressions may be used to verify computer code implementations of ejecta transport given an initial source distribution. We have also used these expressions in the analysis of ejecta transport measurements, for Sn into He gas and a distribution of W particles into Ar and Xe gases. The analysis of these experiments is preliminary, in particular the microsopic analysis of the initial W layer is in progress. The preliminary indications of particulate break-up in the Xe experiments are of particular interest suggesting that experiments which span the gas temperature region below and above the W melting temperature would be of great interest. The solutions presented refer to particle drag only. There are other terms on the right hand side of equation 4 which may modify the transport results. It should also be noted that the thermal transport between particle and gas has not been considered in the equations presented here nor have Mach number effects been included. Nevertheless the agreement between experiment and theory in a minimal model is encouraging.

Acknowledgements

This work was performed under the auspices of the U.S. Department of Energy under contract DE-AC52-06NA25396.

References

1. Zellner, M. B., McNeil, W. V., Hammerberg, J. E., Hixson, R. S., Obst, A. W., Olson, R. T., Payton, J. R., Rigg, P. A., Routley, N., Stevens, G. D., Turley, W. D., Veeser, L., and Buttler, W. T., J. Appl. Phys., **103**, 123502 (2008).

2. Zellner, M.B. et al., to be published.

3. M. B. Zellner, M. Grover, J. E. Hammerberg, R. S. Hixson, A. J. Iverson,G. S. Macrum, K. B. Morley, A. W. Obst, R. T. Olson, J. R. Payton, P. A. Rigg, N. Routley, G. D. Stevens, W. D., W. D. Turley, L. Veeser, and W. T. Buttler, J. Appl. Phys. **102**, 013522 (2007).

4. Germann, T.C., Hammerberg, J.E. and Holian, B.L., "Large-Scale Molecular Dynamics Simulations of Ejecta Formation in Copper", Proceedings of the American Physical Society Topical Group on Shock Compression of Condensed Matter, Portand, Oregon, July 20-25, 2003, pp. 285-288.

5. Germann, T.C., Dimonte, G., Hammerberg, J.E., Kadau, K., Quenneville, J. and Zellner, M.B., "Large-scale molecular dynamics simulations of particulate ejection and Richtmyer-Meshkov instability development in shocked copper", Proceedings of the 9th International Conference on the Mechanical and Physical Behaviour of Materials under Dynamic Loading – DYMAT 2009, Volume 2, 2009, pp. 1499 – 1505. http://dx.doi.org/10.1051/dymat/2009212.

6. Hammerberg, J.E., Plohr, B., Zellner, M.B. and Buttler, W.T., "Particulate Distribution Function Evolution for Ejecta Transport (U)", Proceedings of the 15th Nuclear Explosives Code Developers' Conference, Livermore, California, October 26-30, (2009).